Fachtagung "Lasermethoden in der Strömungsmesstechnik"
9. – 11. September 2014, Karlsruhe

Wind loads on flat boards and walls induced by passing vehicles

Windkräfte auf flache Platten und Wände verursacht durch vorbeifahrende Fahrzeuge

B. Ruck & P. Lichtneger
Laboratory of Building- and Environmental Aerodynamics, Institute for Hydromechanics
Institute of Technology (KIT), Kaiserstr. 12, 76128 Karlsruhe, Germany
Corresponding author: ruck@kit.edu

Keywords: Vehicle, interaction, wind load, board, wall, aerodynamics
Schlagworte: Fahrzeug, Wechselwirkung, Windkraft, Plattenelemente, Wand, Aerodynamik

Abstract
Vehicles of different type pass every day and innumerably roadside-mounted or overhanging flat elements like traffic signs, billboards or charge devices. The vehicle aerodynamics generates a vehicle-specific flow and pressure field, which leads to transient wind loads on these elements. In order to quantify the wind loads, a full-scale measuring campaign with different vehicle types and differently sized testing boards was carried out. The campaign delivered a broad data base for the quantification of wind loads on roadside-mounted or overhanging flat elements allowing a better lay-out of such structures. Additionally, the wind loads induced by different vehicle types on extended walls was investigated in full-scale.

Introduction
Specific pressure and flow fields develop around all moving vehicles. In almost all cases, a first zone of overpressure at the front of the vehicle (bow wave) is followed by a zone of underpressure at the side walls and roof of the vehicle. Thus, an roadside-mounted or overhanging flat element as well as an extended wall experience a resulting pressure force when a vehicle passes. The strength of the transient force depends on the vehicle type and shape, its aerodynamics, the vehicle velocity and the passing distance between vehicle and element/wall. During the vehicle's passing, in the gap between the vehicle and the flat element/wall, a specific highly unsteady flow field develops. Of course, vehicle aerodynamics has been investigated in numerous studies in the last decades, see e.g. Sovran et al. 1978, Hucho 1994, Watkins and Pagliarella 2007 and many others, however, the interaction of the vehicle induced flow with static elements near the road has been investigated barely.
Cali and Covert 2000 performed experiments in a scale of 1:30 by measuring transient loads on overhanging highway signs induced by the passing of simplified vehicle models. Macciacchera and Ruck 2001 conducted investigations in a reduced scale giving detailed pressure measurements near passing vehicles. Full-scale experiments on vehicle induced forces acting on flat plates were carried out by Quinn et al. 2001 a,b. In this case, plates of different shape and inclination were tested on a road side, however, without precise acquisition of vehicle type, distance and travelling speed. Sanz-Andrés et al. 2003 have introduced a mathematical model of vehicle-induced transient loads which roughly approximated experimented results in the bow wave section. In comparison to that, more studies exist on train-induced pressure and suction loads e.g. concerning noise barriers and trackside structures at high speed train lines, where frequent passings can lead to dynamic reactions and/or material fatigue, see e.g. Baker et al. 2001, Sterling et al. 2008, Friedl et al. 2013, Lee 2009 or Carassale and Brunenghi 2013. Also cross wind and gust induced effects on vehicles and road-

side structures were treated in several studies in model as well as in full scale experiments, see e.g. Pulipaka et al. 1998 or Dorigatti et al. 2012.
Summarizing the existing knowledge in the field of interaction of vehicle induced flow with static elements near the road leads to the conclusion that no data of systematic investigations exist respecting all, the element size and alignment, vehicle type, passing distance etc. In order to fill this gap of knowledge, the present project was realized consisting of the following steps:

- A wind tunnel study with truck models using LDA technique to infer the undisturbed flow field around trucks and to be able to correlate it with the obtained pressure results from the following extensive full-scale measurements.

- A full-scale measurement campaign performed with different vehicle types on a closed road section with numerous configurations and positions of three individual testing boards. For all configurations and positions, the aerodynamic interaction, i.e. the vehicle induced loads were measured.

- A full-scale measurement campaign performed with six vehicle types on a closed road section with a wall-like configuration with a surface-embedded vertical line of pressure sensors to infer the pressure loads induced by passing trucks.

- Setting up a database named VIPAS (**V**ehicle **I**nduced **P**ressure **A**nd **S**uction), which contains typical time series of vehicle induced forces depending on the element configuration, the vehicle type and the passing distance in order to allow a safer design of roadside elements.

Experimental details

Flow field around moving vehicle
As can be seen from Fig. 1, the flow field of realistic truck models of scale 1:16 has been investigated in a wind tunnel study by LDA. A 2D fiber-coupled LDA-system with an argon-ion laser (514 nm and 488 nm) and a sending lens of 1139 mm focal length was used. The investigations were performed in a Göttinger-type wind tunnel with low turbulence intensity (< 1%). The trucks have been fixed at the beginning of a short splitter plate so that the forming boundary layer above the plate was very thin.

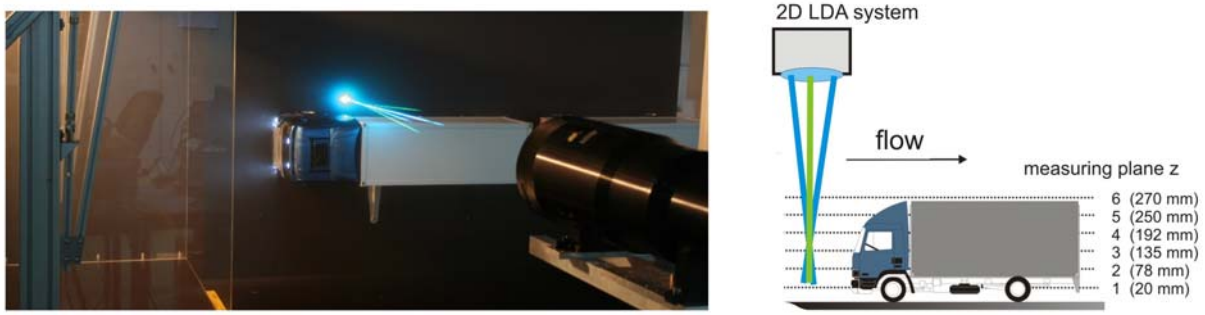

Fig. 1: Wind tunnel study with truck models in scale 1:16

As can be inferred from Fig. 2, a moving vehicle displaces the quiescent air. Most interesting in this respect is that for near passing distances the wind velocity V measured perpendicular to the direction of movement is about twice as high as the velocity U measured at the same point but in the direction of vehicle movement.

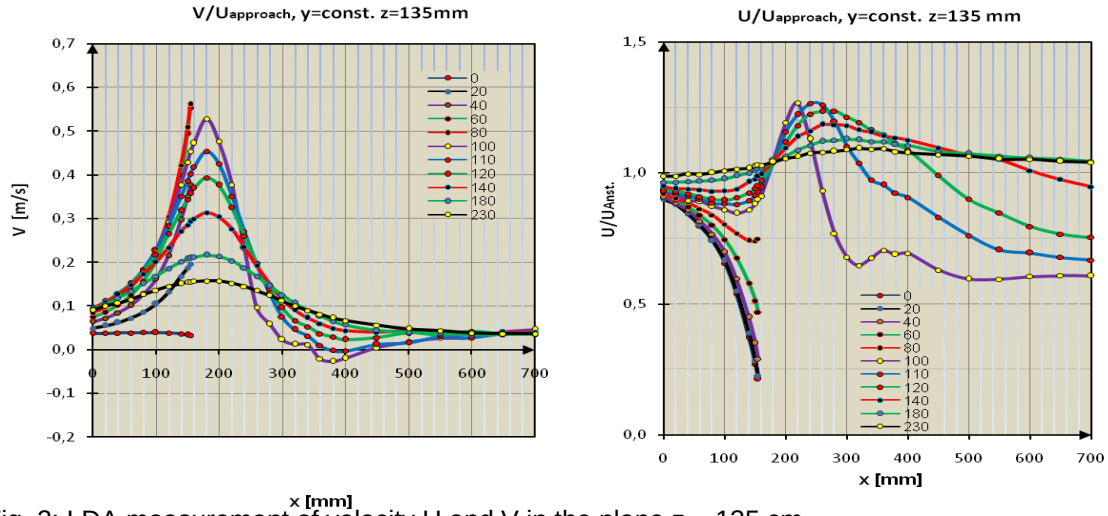

Fig. 2: LDA measurement of velocity U and V in the plane z = 135 cm

Since most of the European trucks, typically, have a box shape the measurements differ only slightly between the trucks of different truck manufacturers.

Full-scale measurements with testing boards

Fig. 3 explains the full-scale measurements with differently sized testing boards and denotes the parameters of influence.

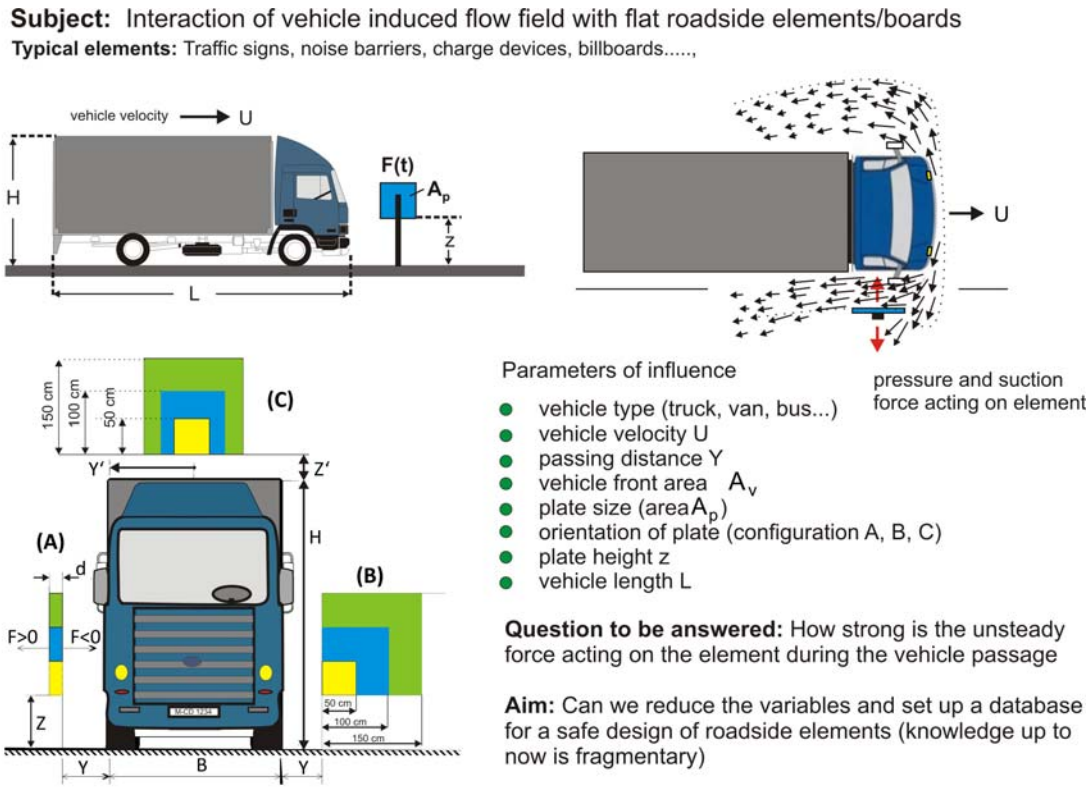

Fig. 3: Three different testing boards (50 cm X 50 cm, 100 cm X 100 cm, 150 cm X 150 cm, denoted as small-sized, medium-sized and large-sized board) with three different configurations (board alignments)

The measurements were performed on a straight road section of 800 m length having two turning loops at the ends, see Fig. 4. Two containers with electronic control and data

processing units including a weather station were installed near-by. The atmospheric wind conditions were registered parallel to all measurements to exclude non-vehicle wind load contributions. In order to fix the boards at pre-defined y,z-positions a gantry and a fork-lift was used. Vibrations of the boards have been suppressed as much as possible, i.e. the rocking forces should be measured and not the plate dynamics.

Fig. 4: Test field and measuring devices

Hundreds of test runs were performed with different vehicle types, see Fig. 5, and for different so-called test positions. A test position was defined as a combination of one particular configuration, vehicle type and vertical level Z of the test plate. At each test position, typically, N = 15 to 25 test runs were carried out.

vehicle type	total width B [m]	total height H [m]	total length L [m]	characteristics			examples	
passenger car (saloon)	1.75	1.45	4.5 - 4.8	combined lim./ estate				
van (commercial vehicle)	2.0	2.7	5.4/6.8	combined short/long				
truck (goods vehicle)	2.5	3.4	7.8	rigid box body				
truck with trailer (road train)	2.6	4.0 (3.55)	16.6	canvas cover, trailer lower				
trailer-truck (articulated vehicle)	2.6	4.0	16.6 - 18.6	canvas cover				
tour-bus (long distance coach)	2.55	3.7	12.95	3-axle, roof structures				

Fig. 5: Vehicle fleet consisting of six different vehicle types

For each run, the variable vehicle velocity U and the variable distance Y between plate and vehicle were captured automatically using laser light beam trigger and distance measuring technique. The testing boards were equipped with many pressure tappings on both sides, see Fig. 6, in order to measure differential pressure distributions with high spatial and temporal resolution during the vehicle's passing. Integrating the instantaneous differential pressure distribution leads to a transient force acting on the element, which is a function of vehicle type, passing distance Y, vehicle velocity U and time t. Two different embedded pressure scanning systems were used for the experiments. Small- and large-sized plates were equipped with a digital temperature compensated DTC Initium System from Measurement Specialties with 2 miniaturized electronic scanners ESP32HD, each with 32 silicon piezoresistive pressure sensors and a nominal accuracy of ± 0.06 % FS with FS = ± 2.5 kPa and a data rate of 1 kHz per channel. Both ESP scanning arrays were implemented opposite to each other on both surfaces of the plate. Shearing the common reference pressure of both EPSs, the differential pressure could be computed directly in a grid of 30 (small-sized plate) and 32 (large-sized plate) taps. The medium-sized plate was equipped with a high speed USB-2537 DAQ board from MCC and an array of 64 analog signal conditioned and temperature compensated differential pressure transducers HCX from Sensortechnics, having a nominal accuracy ± 0.1 %FS with FS = ± 1 kPa and a data rate 3 kHz per channel.

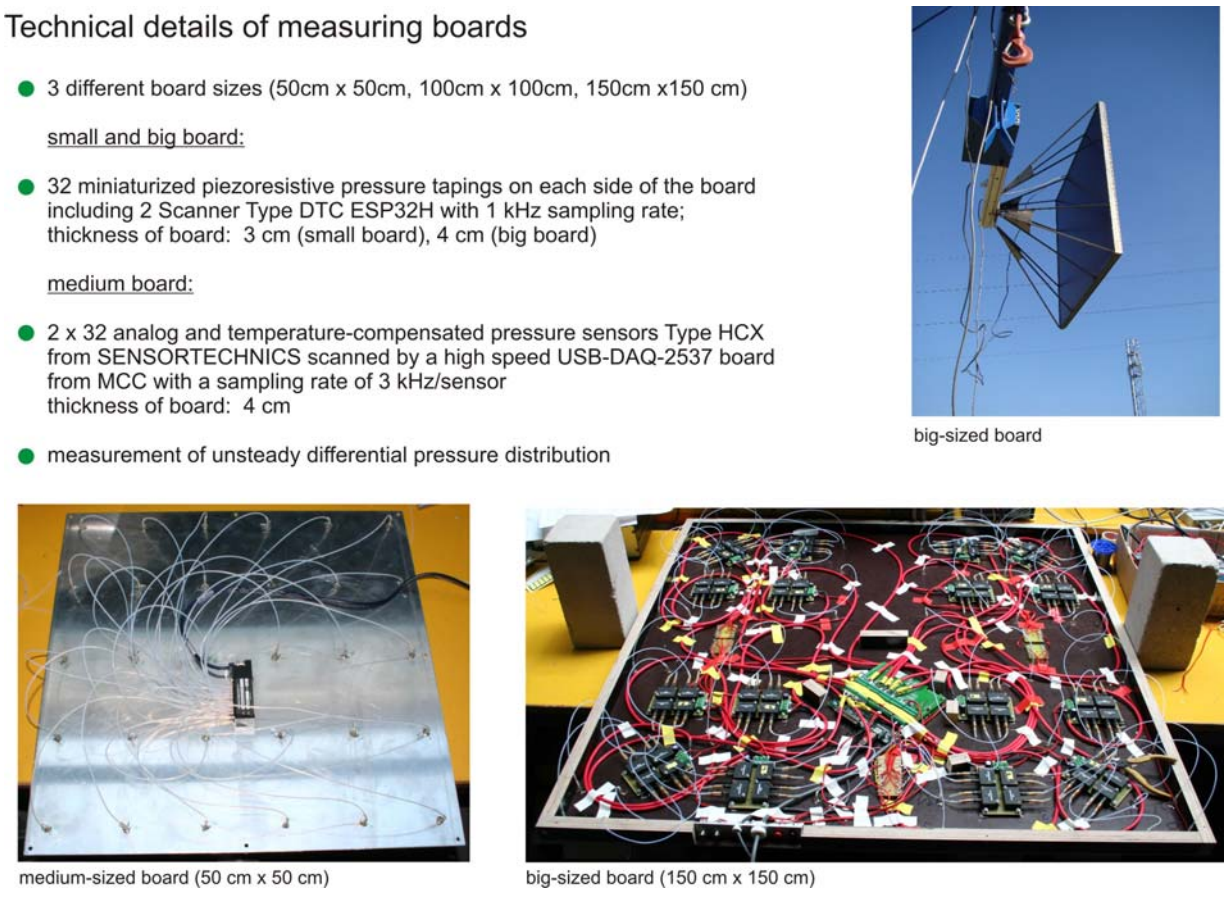

Fig. 6: Testing boards with embedded pressure scanning systems

The data capturing and processing was performed on the basis of individual force curves (integration of the instantaneous differential pressure distribution in the boards). Considering one vehicle type, hundreds of force curves were detected, which differ in amplitude and temporal length according to the fact that not all tested vehicles of this type had the same veloci-

ty and the same distance with respect to the testing board, see also Fig. 7, where the data processing is explained. In order to decrease the variety of force curves and to reduce the variables, first of all, the vehicle-induced force F(t) was normalized by a force consisting of the product of vehicle velocity-based dynamic pressure, air density and the vehicle frontal area (A_v = B x H). This led to the dimensionless transient force coefficient $C_F(t)$. The curves for the dimensionless transient force coefficient C_F (t) still depend on U and Y, however, all curves of the same passing distance show now the same amplitude but have different time durations due to varying vehicle velocity. If we introduce on the abscissa a dimensionless time t_n formed by multiplying the real time with the vehicle velocity divided by the vehicle length L, then, all measured curves of the dimensionless transient force coefficient $C_F(t_n)$ will have the same length. Thus, for a fixed passing distance Y, the curves of $C_F(t_n)$ show the same amplitude and length, i.e. $C_F(t_n)$ depends only on Y. Since the dimensionless transient force coefficient $C_F(t_n)$ depends only on Y, it should be possible to divide it by a function k(Y), which is called 'distance model', forcing all curves collapsing to more or less one single curve, the so-called 'characteristic load curve' $C_F^*(t_n)$ for one test position, see Fig. 7.

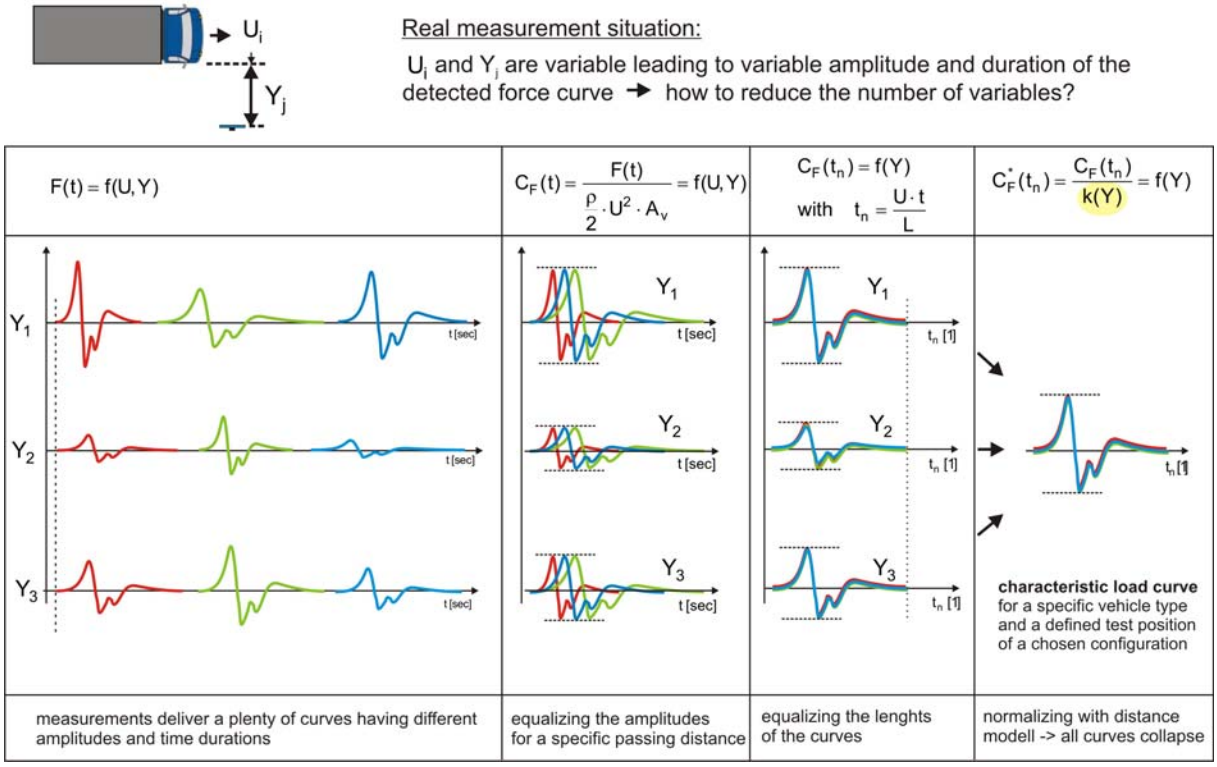

Fig. 7: Data processing and characteristic load curve

A distance model describes the relation between force impact and passing distance Y. In order to obtain a distance model, a great number of vehicle passings was realized with a specified test position measuring the differential force coefficient (difference of the force coefficient of the first maximum P1 and first minimum P3) in each curve, see Fig. 8. Applying the procedure in Fig. 8 yielded the characteristic load curves, which could be obtained for each test position and which were fed into a database named VIPAS, see Fig. 9. The use of database VIPAS is explained in Fig. 10 with a typical data set. Beside the characteristical load curves, the user can download video sequences showing the unsteady differential pressure distribution in the boards. Based on these data also a resulting moment can be deduced for any position of an axis of rotation. Furthermore, comparative plots can be seen and downloaded for one fixed board alignment but different vehicle types.

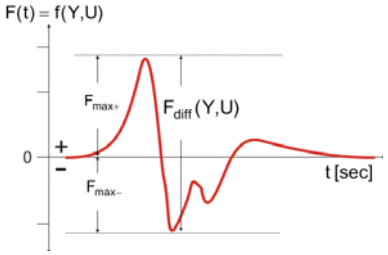

Shape of distance model

$$k(Y) = a \cdot (Y + b)^{-3}$$

It was found that the differential force coefficient $C_{F,diff13}$ could be approximated with a -3rd* power function fitted within the tested distance range. Thus, for each test position, a distance model k(Y) was estimated applying model coefficients a [m³] and b [m] appropriately.

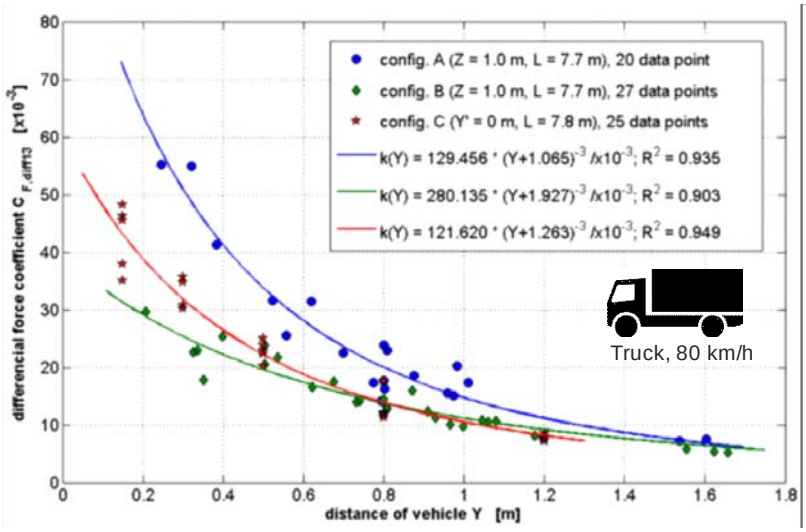

➔For each combination of vehicle type, board size, position and orientation, a distance model could be deduced

Fig. 8: Differential force coefficient (characterizing the force jump between the first maximum and first minimum of a detected force curve) depending on passing distance of vehicle with respect to testing plate. Fitting of curves (distance models) to the measurement values for three truck test positions (for configuration C, the notation of distance Y symbolizes vertical distance Z'); R^2 coefficient of determination

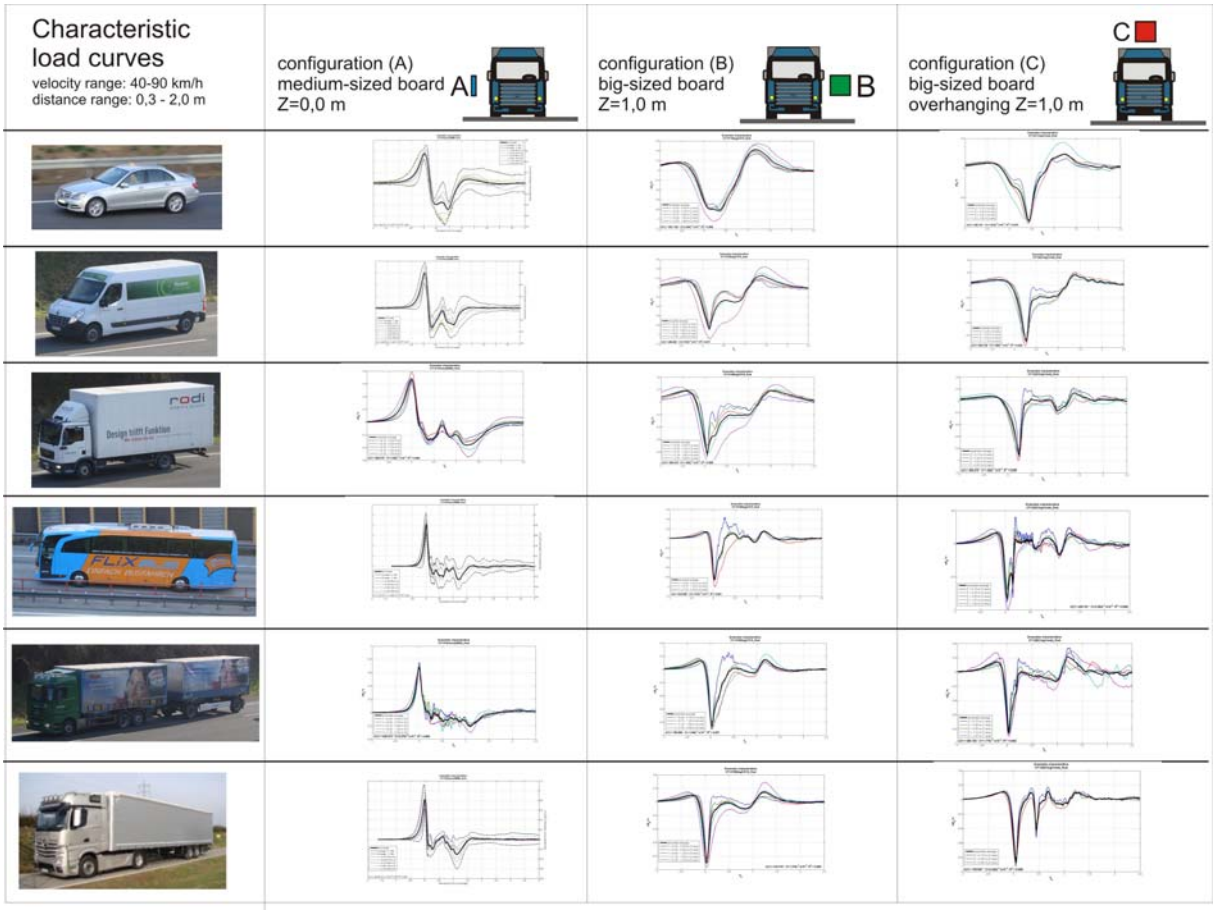

Fig. 9: Examples of characteristic load curves (can be found in database VIPAS) for different vehicle types and board alignment)

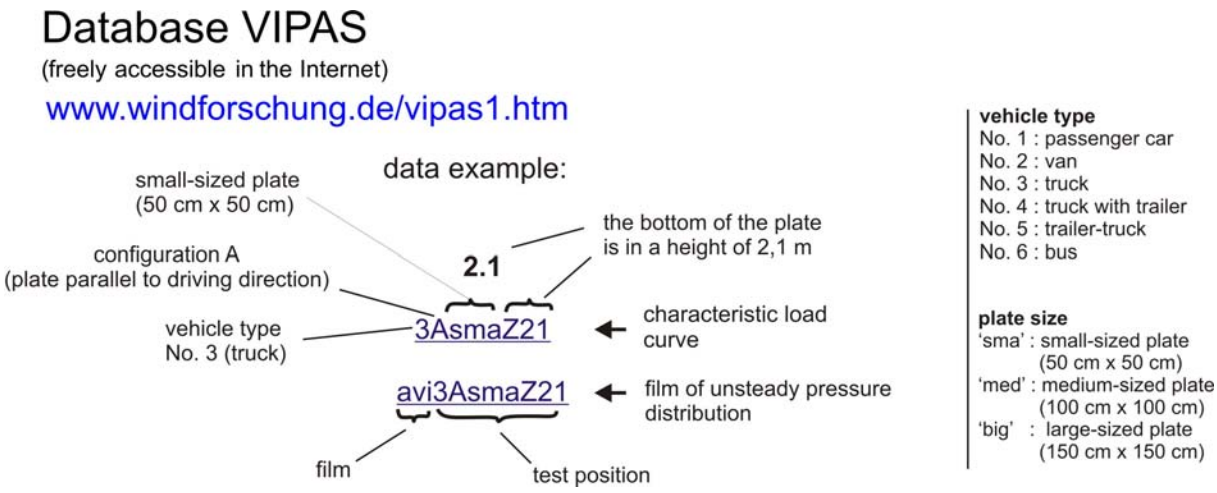

Fig. 10: Data notation in database VIPAS

Adequate normalizing, plotting against a dimensionless time and the deduction of distance models allowed the generalization of the data being valid now also for other not measured vehicle velocities and passing distances. Thus, for a fixed vehicle type, board configuration and position, the loads can be computed for user defined velocities and passing distances. Supposed, the passing distance Y, the vehicle velocity U and the vehicle type with frontal area A_v are known, the data base VIPAS can be used to compute the wind load F(t) or F(X) acting on a flat element of size 50 cm x 50 cm, 100 cm x 100 cm or 150 cm x 150 cm in height Z with configuration A, B or C. This computation can be performed on the basis of the experimentally determined characteristic load curves $<C_F^*>$ in combination with the distance models k(Y) derived from full scale measurements:

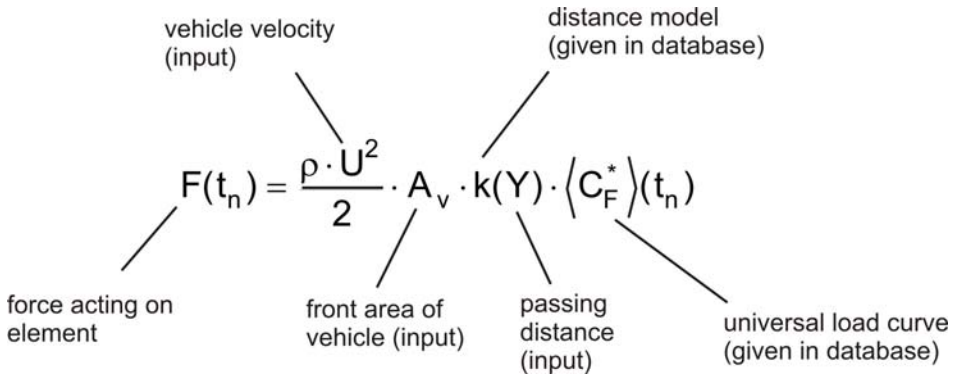

In this way, comparative plots can be computed for exactly the same vehicle velocity and passing distance of all investigated vehicle types, see example in Fig.11.

Full-scale measurements with wall-like configuration

When vehicles move close to extended walls, a characteristical pressure imprint of the vehicle type moves over the wall. To investigate the induced load behaviour, systematic full scale investigations have been carried out also for this case. The wall was realized with stacked oversea containers, see Fig. 12 and 13, where further experimental details are revealed. In Fig. 14, typical pressure imprints of four different vehicle types are shown. The evaluation of the measured data is underway and we aim at setting up part 2 of database VIPAS, which allows for a specific vehicle type the computation of pressure at any point of the wall as a function of vehicle velocity and passing distance.

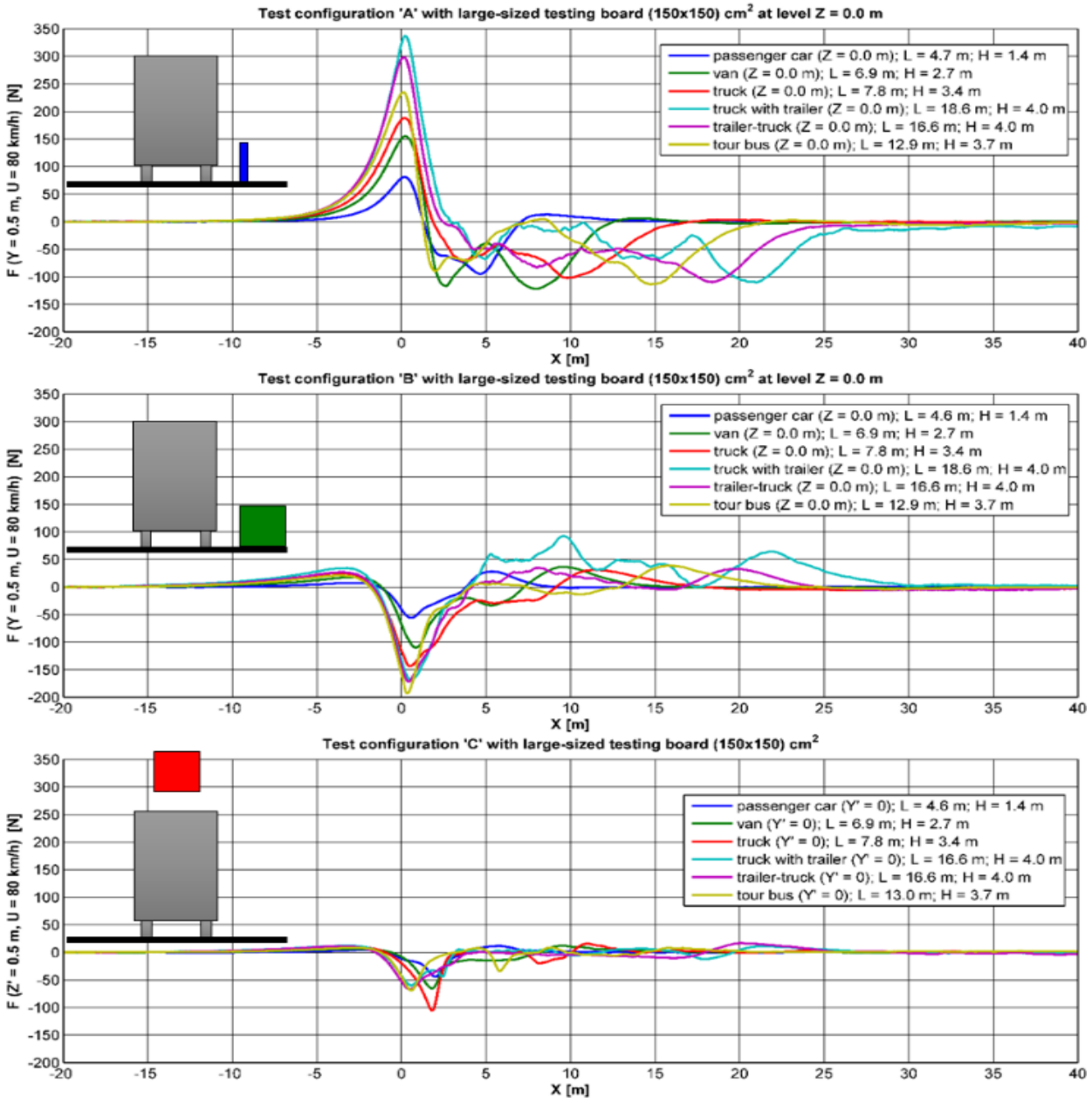

Fig. 11: Characteristic vehicle-induced resultant force on the large-sized testing plate with a passing distance of 0,5 m and a passing velocity of 80 km/h for all three configurations

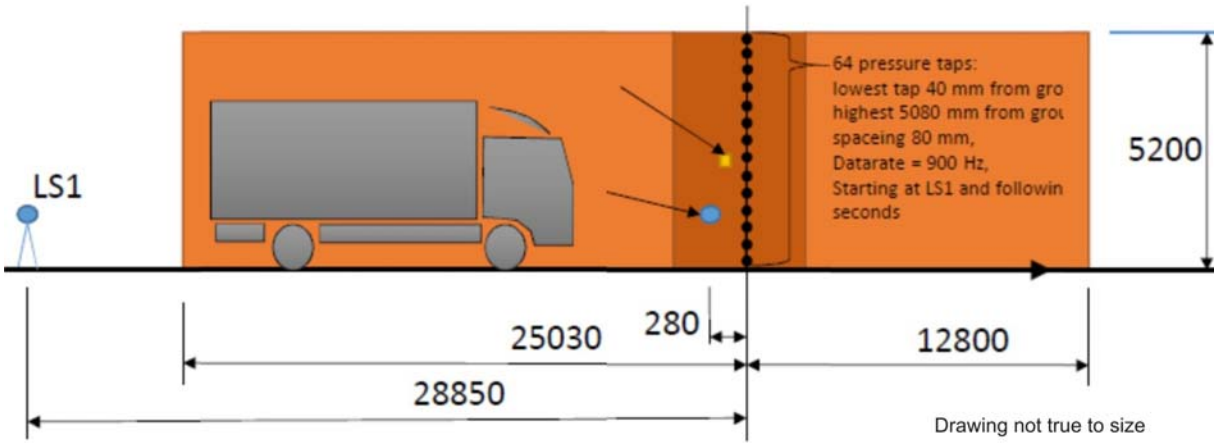

Fig 12: Sketch of full-scale measurements with wall-like configuration

Fig. 13: Vehicle passages at extended walls with different vehicle types

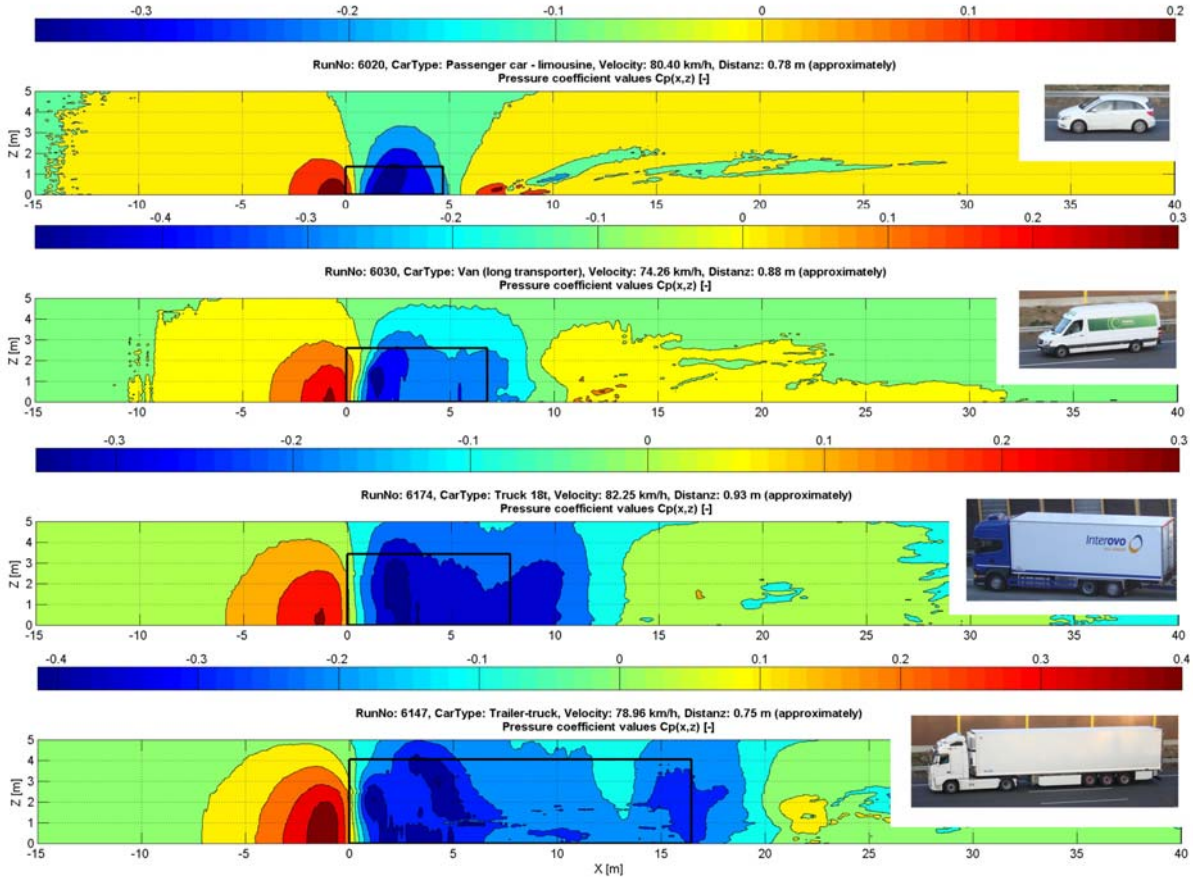

Fig. 14: Typical pressure imprints of moving vehicles of different type at extended walls

Acknowledgement

The authors gratefully acknowledge the financial support of the German Research Foundation for this project (DFG research grant No. Ru-345/32-1). We thank Dr.-Ing. Boris Pavlovski for performing the LDA measurements.

References

Baker, C. J., Dalley, S. J., Johnson, T., Quinn, A., Wright, N. G., 2001: The slipstream and wake of a high-speed train, Proceedings of the Institution of Mechanical Engineers, Part F: Journal of Rail and Rapid Transit, 215 (2), 83 - 99, DOI: 10.1243/0954409011531422

Cali, P. M., E. E. Covert, 2000: Experimental measurements of the loads induced on an overhead highway sign structure by vehicle-induced gusts, Journal of Wind Engineering and Industrial Aerodynamics, vol. 84: pp. 87-100

Carassale, L., Brunenghi, M.M., 2013: Dynamic response of trackside structures due to the aerodynamic effects produced by passing trains, J. WindEng. Ind. Aerodyn., 123, pp. 317–324

CEN 2005: EN 14067: Railway Applications - Aerodynamics.

Dorigatti, F., Sterling, M., Rocchi, D.,Belloli, M., Quinn, A.D., Baker, C.J.,Ozkan, E., 2012: Wind tunnel measurements of crosswind loads on high sided vehicles over long span bridges, Journal of Wind Engineering and Industrial Aerodynamics, 107-108, pp. 214-224

Friedl, H., Reiterer, M., Kari, H., 2013: Analysis of aerodynamic impact induced by high speed trains, Proc. of Fourth international conference on civil, structural and environmental engineering computing. B. H. V. Topping and P. Iványi, Civil-Comp Press.

Hucho, W.-H. (Ed.), 1994: Aerodynamik des Automobils, VDI Verlag Düsseldorf, ISBN 3-18-400970-X

Lee, H. S.-H., 2009: Safety of High-Speed Ground Transportation Systems : The aerodynamic effects of passing trains to surrounding objects and people, U.S. Department of Transportation

Macciacchera, I., Ruck, B., 2001: Pressure fluctuations induced by road vehicles in ambient air - a model study, Workshop on physical modelling of environmental flow and dispersion, Hamburg, University Hamburg

Pulipaka, N., Sarkar, P.P., McDonald, J.R., 1998: On galloping vibration of traffic signal structures, Journal of Wind Engineering and Industrial Aerodynamics, 77-78, pp. 327-336

Quinn, A. D., Baker, C.J., Wright, N.G., 2001 a: Wind and vehicle induced forces on flat plates - Part 1: Wind induced force, Journal of Wind Engineering and Industrial Aerodynamics, vol. 89: 817-829.

Quinn, A. D., Baker, C.J., Wright, N.G., 2001 b: Wind and vehicle induced forces on flat plates - Part 2: Vehicle induced force, Journal of Wind Engineering and Industrial Aerodynamics, vol. 89: pp. 831-847.

Sanz-Andrés, A., Santiago-Prowalda, J., Baker, C., Quinn, A., 2003: Vehicle induced loads on traffic sign panels, Journal of Wind Engineering and Industrial Aerodynamics, Volume 91, Issue 7, Pages 925–942

Sanz-Andrés, A., Laverón, A., Quinn, A., 2003: Vehicle induced loads on pedestrian barriers', Journal of Wind Eng. & Ind. Aerodyn., 92, pp. 413-442

Sovran, G., Morel, T., Mason, W.T. Jr., (Eds.), 1978: Aerodynamic drag mechanisms of bluff bodies and road vehicles, Plenum Press New York, ISBN 0-306-31119-4.

Sterling, M., Baker,C. J., Jordan, S. C., Johnson, T., 2008: A study of the slipstreams of high-speed passenger trains and freight trains, Proceedings of the Institution of Mechanical Engineers, Part F: Journal of Rail and Rapid Transit 2008 222: 177, DOI: 10.1243/09544097JRRT133

Watkins, G. and R. Pagliarella, 2007: The flow environment of road vehicles in winds and traffic. The aerodynamics of heavy vehicles II: Trucks, buses and trains, Springer Berlin Heidelberg